Hearing Research xxx (2016) 1–12

Contents lists available at ScienceDirect

Hearing Research

journal homepage: www.elsevier.com/locate/heares

Research paper

Loudness and pitch perception using Dynamically Compensated Virtual Channels

Waldo Nogueira [a, *], Leonid M. Litvak [b], David M. Landsberger [c], Andreas Büchner [a]

[a] Medical University Hannover, Cluster of Excellence "Hearing4all", Hannover, Germany
[b] Advanced Bionics LLC, Valencia, CA, USA
[c] New York University School of Medicine, New York, NY, USA

ARTICLE INFO

Article history:
Received 10 June 2016
Received in revised form
26 November 2016
Accepted 29 November 2016
Available online xxx

Keywords:
Cochlear implant
Finite element model
Focused stimulation
Current steering
Strategy
Loudness
Pitch

ABSTRACT

Reducing power consumption is important for the development of smaller cochlear implant (CI) speech processors. Simultaneous electrode stimulation may improve power efficiency by minimizing the required current applied to a given electrode. Simultaneous in-phase stimulation on adjacent electrodes (i.e. virtual channels) can be used to elicit pitch percepts intermediate to the ones provided by each of the physical electrodes in isolation. Virtual channels are typically implemented in monopolar stimulation mode, producing broad excitation patterns. Focused stimulation may reduce the excitation patterns, but is inefficient in terms of power consumption. To create a more power efficient virtual channel, we developed the Dynamically Compensated Virtual Channel (DC-VC) using four adjacent electrodes. The two central electrodes are current steered using the coefficient α ($0<\alpha<1$) whereas the two flanking electrodes are used to focus/unfocus the stimulation with the coefficient σ ($-1<\sigma<1$). With increasing values of σ, power can be saved at the potential expense of generating broader electric fields. Additionally, reshaping the electric fields might also alter place pitch coding.

The goal of the present study is to investigate the tradeoff between place pitch encoding and power savings using simultaneous electrode stimulation in the DC-VC configuration. A computational model and psychophysical experiments in CI users have been used for that purpose.

Results from 10 adult Advanced Bionics CI users have been collected. Results show that the required current to produce comfortable levels is significantly reduced with increasing σ as predicted by the computational model. Moreover, no significant differences in the estimated number of discriminable steps were detected for the different values of σ. From these results, we conclude that DC-VCs can reduce power consumption without decreasing the number of discriminable place pitch steps.

1. Introduction

Cochlear implants (CIs) are implantable medical devices that are used to restore the sense of hearing for people with profound hearing loss or deafness. Over the past few decades, the CI sound processor has been extensively developed to improve speech intelligibility outcomes (Wilson et al., 1991; Loizou, 1998; Wouters et al., 2015). With current technology, CI users tend to have good speech recognition in quiet but have difficulty in understanding speech in more difficult listening environments. Additionally, the size of the CI sound processor has been greatly reduced. Nevertheless, both performance with the CI and size of the sound processor still need to be improved. Because the batteries limit miniaturization of the sound processor, it is crucial to design strategies and implants that more efficiently use power while maintaining or improving performance.

Current CI systems require the user to wear an external device with batteries, microphone, sound processor, and transmitting coil to power and control the internal device. Both the internal and external components are powered by the batteries in the speech processor. Low power consumption is required to miniaturize the CI batteries and to provide smaller CI sound processors (Mertens et al., 2015) or to achieve the long-term goal of a fully implantable system (Briggs et al., 2008). For this reason, new developments in CIs often try to reduce power consumption without compromising speech intelligibility and quality. One possibility to achieve

* Corresponding author.
E-mail address: nogueiravazquez.waldo@mh-hannover.de (W. Nogueira).

http://dx.doi.org/10.1016/j.heares.2016.11.017
0378-5955/© 2016 Published by Elsevier B.V.

Abbreviations

3D	Three Dimensional
AFC	Alternative Forced Choice
ANOVA	Analysis of Variance
CI	Cochlear Implant
CIS	Continuous Interleaved Sampling
DC-VC	Dynamically Compensated Virtual Channel
ELC	Equal Loudness Contour
FEM	Finite Element Method
MPVC	Monopolar Virtual Channel
QPVC	Quadrupolar Virtual Channel
TP	Tripolar
VC	Virtual Channel

low power consumption consists of minimizing the supply voltage of the implant (Zeng et al., 2008). The supply voltage, which depends on the maximum current delivered to the electrode contacts and their corresponding impedances, needs to be higher than the maximum voltage required to achieve comfortable loudness. For this reason, stimulation modes requiring low currents and low impedances are desired.

One limitation of CIs is the limited spectral information that they deliver. Although only 4 spectral channels are required to understand speech in quiet (Shannon et al., 1995), speech perception in more difficult listening conditions requires more spectral channels (Shannon et al., 2004). Spectral information is probably limited by the channel interactions created when different electrodes stimulate overlapping populations of neurons (e. g. Fu and Nogaki, 2005). Reducing the spread of excitation from a stimulated electrode could narrow the population of activated neurons and can potentially reduce channel interactions across electrodes. Speech intelligibility in noise may be improved by reducing electric and neural interactions across electrodes which in theory should improve spectral resolution (e.g. Henry et al., 2000; Litvak et al., 2007).

Multiple electrode stimulation can also be used to elicit several pitches intermediate to the pitches provided by the physical electrodes (e.g. Firszt et al., 2007; Landsberger and Galvin, 2011) using monopolar virtual channels (MPVCs). In a MPVC, the current field is steered between the physical electrodes according to a parameter α, which ranges from 0 to 1 and represents the proportion of current delivered to the more basal physical electrode (see Fig. 1). For example, if $\alpha = 0$, all of the current is delivered to the apical electrode; if $\alpha = 1$, all of the current is delivered to the basal electrode; if $\alpha = 0.5$, 50% of the total current is delivered to each of the physical electrodes. Electrical models of the human cochlea and psychoacoustic experiments have shown that VCs delivered through simultaneous stimulation are generally able to produce a single, gradually shifting intermediate pitch (Frijns et al., 2009; Luo et al., 2010, 2012). Evoked compound action potential (ECAP) measures (Busby et al., 2008; Hughes et al., 2013) and modeling (Litvak et al., 2007) suggest that the current spread from a MPVC is similar to that of MP stimulation on a single electrode. VCs have been implemented in Advanced Bionics' Fidelity 120 speech processing strategy, with no clear advantage in speech perception (Buechner et al., 2008) or spectral resolution (Berenstein et al., 2008) over the standard 16-channel continuous interleaved sampling (CIS) strategy. These results may be explained by the fact that channel interactions due to current spread may limit the spectral resolution with VCs to a similar degree as with physical electrodes.

Improvements in spectral resolution performance can be obtained using current focusing to reduce channel interaction. One current focusing implementation is tripolar stimulation (TP; e.g., Litvak et al., 2007; Berenstein et al., 2008; Bierer and Faulkner, 2010; Landsberger et al., 2012). With TP stimulation, an active electrode is stimulated and the two flanking (ground) electrodes are stimulated in opposite polarity phase relative to the active electrode, with each receiving half the current of the active electrode (see Fig. 1). Physiological (e.g. Bierer and Middlebrooks, 2002), computational (e.g. Spelman et al., 1995; Briaire and Frijns, 2010; Litvak et al., 2007), and psychophysical (Bierer and Faulkner, 2010; Landsberger et al., 2012; Fielden et al., 2013; Padilla and Landsberger, 2014) studies have shown that TP stimulation reduces current spread compared to MP stimulation. Current focusing can be implemented in combination with virtual channels. One example of a current focused virtual channel is the quadrupolar virtual channel (QPVC, Landsberger and Srinivasan 2009; Srinivasan et al., 2012). QPVCs are created by simultaneously stimulating four adjacent electrodes (see Fig. 1). The middle two electrodes are used for current steering, similarly to MPVCs. The remaining two flanking electrodes are used as grounds or partial-grounds to focus the stimulation, reducing current spread, similarly to TP stimulation. However, as previously mentioned, maintaining a fixed loudness with focused stimulation requires much greater current than with MP stimulation. Even with large phase durations (which ultimately limit the stimulation rate), it is difficult to achieve maximally acceptable loudness (Landsberger and Srinivasan, 2009).

It is worth noting that the benefits of current focusing are still unclear. Two studies (Landsberger and Srinivasan, 2009; Srinivasan et al., 2012) have shown that adding current focusing to a virtual

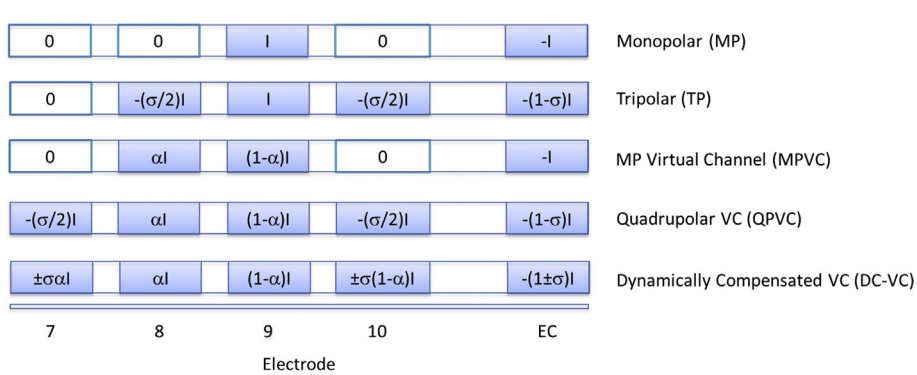

Fig. 1. Illustration of different stimulation modes. The sign indicates the polarity and the absolute value indicates the magnitude of the current provided on the corresponding electrode. The x-axis describes the electrode position (EC = extra-cochlear electrode). Note that the sign of σ in Landsberger and Srinivasan (2009) is inverted.

Please cite this article in press as: Nogueira, W., et al., Loudness and pitch perception using Dynamically Compensated Virtual Channels, Hearing Research (2016), http://dx.doi.org/10.1016/j.heares.2016.11.017

channel can improve virtual channel discrimination. Berenstein et al. (2008) and Smith et al. (2013) both demonstrate improved spectral resolution with a current focused strategy. Although current focusing seems to improve spectral resolution, the benefit of current focusing on speech in noise is less clear. Berenstein et al. (2008) found no consistent benefit for speech in noise with TP stimulation over MP stimulation. However, the TP strategy for four out of nine subjects used a current focusing coefficient (σ) of 0.25 which would be expected to provide a spread of excitation very similar to an equally loud MP stimulus (Bierer and Middlebrooks, 2002; Bonham and Litvak, 2008; Landsberger et al., 2012). All subjects in Srinivasan et al. (2013) provided better speech in noise performance with a TP strategy than with a MP strategy. Bierer and Litvak (2016) also observed an improved performance with TP strategies over MP strategies for poorer performing subjects.

The challenge is therefore to design sound coding strategies that optimize both power consumption and sound performance. One possibility to optimize power is to use multiple simultaneous electrode stimulation (e.g. Donaldson et al., 2005; Busby et al., 2008). For a given rate and amplitude the loudness perception produced by multiple electrode stimulation is greater than that of a single electrode activated at the same rate and level (McKay et al., 2001). This loudness increase may be explained by the contribution of each electrode to the others by the current spread phenomenon.

In an attempt to simultaneously optimize discriminability of VCs and power consumption, a new stimulation mode has been created (Litvak and Marzalek, 2012). This mode uses simultaneous stimulation of four adjacent electrodes similarly to QPVC stimulation (see Fig. 1). The two central electrodes are current steered using the coefficient α ($0<\alpha<1$) whereas the two flanking electrodes are used to focus/unfocus the stimulation with the coefficient σ ($-1<\sigma<1$). With this stimulation mode the sign of σ is opposite to what is used in QPVC i.e. $\sigma<0$ is focused. Another difference between these two stimulation modes is that in the new mode the flanking electrodes are also multiplied by the current steering coefficient. Specifically, the electrodes (ordered from apical to basal) provide the following currents: $I\alpha\sigma$, $I\alpha$,$I(1-\alpha)$,$I(1-\alpha)\sigma$. With increasing values of σ, power can be saved at the potential expense of generating broader electric fields. It is worth noting that when $\sigma=0$ a DC-VC is physically identical to a MPVC.

One suggestion to incorporate this new stimulation mode in a sound coding strategy is to use focused stimulation for soft sounds and unfocused stimulation for loud sounds (Fig. 2). By doing so, at soft levels it is possible to deliver more focused stimulation without compromising power savings. For loud sounds however, large electrical stimulation currents are possible, and therefore power can be saved using unfocused stimulation. Because the amount of compensation is dynamically adjusted we termed this stimulation mode the Dynamically Compensated Virtual Channel (DC-VC).

It is unknown how DC-VC effects power consumption and spectral resolution. In the present study, DC-VC stimulation is investigated in two main experiments related to loudness and pitch perception. The first experiment studies loudness perception for different values of the focusing coefficient σ and the current steering coefficient α. This study has relevance for the development of sound coding strategies based on current steering because these strategies require constant loudness perception across the current steering coefficient α to properly encode place pitch (Frijns et al., 2009; Nogueira et al., 2009). The second experiment aims to understand how pitch changes as a function of the current steering coefficient α and the focusing coefficient σ. Both experiments are supported by a computational model that simulates intra-cochlear potential fields and auditory nerve responses produced by DC-VC stimulation. The electric fields and the associated nerve responses

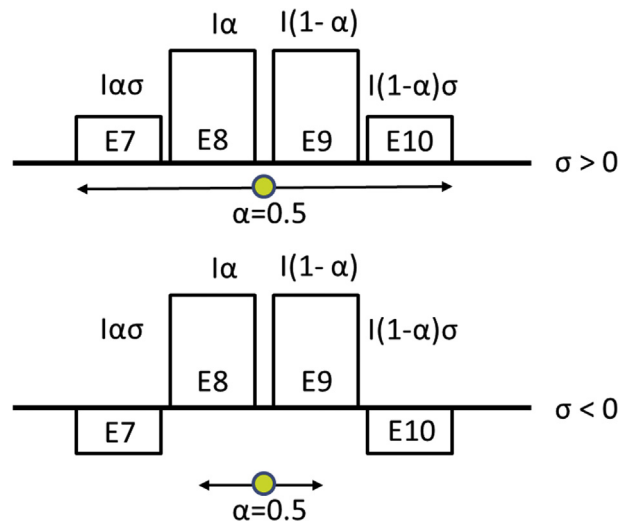

Fig. 2. Schematic illustration of dynamic compensated-virtual channels (DC-VC) stimulation mode. The parameters α and σ determine the current distribution on the four electrodes being combined to one channel. The unfocused version of DC-VC stimulation is shown on the top whereas the focused version is shown on the bottom. The green dot indicates the estimation of the peak of the overall voltage distribution created by DC-VC stimulation. The horizontal arrow indicates the range of locations the peak can take varying the parameters α and σ. (For interpretation of the references to colour in this figure legend, the reader is referred to the web version of this article.)

are used to model pitch and loudness perception for different configurations of DC-VC stimulation.

1.1. Experiment 1: loudness perception with Dynamically Compensated Virtual Channels

1.1.1. Loudness model

A computational model has been designed to make quantitative predictions of loudness and pitch perception using the DC-VC mode (Nogueira et al., 2016). Computational models have been successfully used to investigate multipolar stimulation in the implanted cochlea (e.g. Litvak et al., 2007; Frijns et al., 2011; Snel-Bongers et al., 2013; Wu and Luo, 2013; Kalkman et al., 2014). Modeling studies are less time-consuming than testing human CI users. They can provide valuable insights into human perceptual data because of their capability to adjust specific CI factors and examine conditions that are difficult to test in real CI users. The purpose of our computational model is to generate and support hypotheses concerning the mechanisms underlying loudness and pitch perception elicited by DC-VC by comparing the model outcomes to experimental psychophysical results from CI users. As stimulation modes become more complicated, the fitting of these modes into a sound coding strategy becomes more complex.

The model used in this manuscript is composed of two parts: an electrical field model and a neural activity model. Similar to the model of Litvak et al. (2007), the model assumes the following: (1) there exists a finite number of discrete neuronal elements spread out over the cochlear space, (2) these elements have a range of thresholds drawn from a log-normal distribution. Moreover, the new model assumes that the electric field at a given spatial location is obtained from a finite element method (FEM) simulation, unlike the model of Litvak et al. (2007).

The spread of electric current in the cochlea is simulated in a 3D FEM. The geometry of the cochlea containing the scala tympani, scala vestibuli, reissner membrane, basilar membrane, the modiolus and the nerve is constructed from a single microphotography

Please cite this article in press as: Nogueira, W., et al., Loudness and pitch perception using Dynamically Compensated Virtual Channels, Hearing Research (2016), http://dx.doi.org/10.1016/j.heares.2016.11.017

slice (Fig. 3a) following a method similar to the one introduced by Rattay et al. (2001). The compartments from the single slice are interpolated every 90° using splines to comprise two and a half turns of the cochlea. A spline interpolation of the auditory nerve compartment is used to create 10,000 nerve fibers along the cochlea.

The 3D computer assisted drawing (CAD) model was generated in Inventor© and imported into COMSOL© (COMSOL Group, Stockholm, Sweden) to generate a tetrahedral mesh using the general physics algorithm. Three different meshes with different levels of refinement were generated for a mesh convergence study. The minimum element sizes were $5\cdot10^{-4}$, $2\cdot10^{-4}$ and $7.5\cdot10^{-5}$, and the total numbers of elements were 16,229, 309,670 and 387,451 for each level of refinement. Each compartment was assigned a material property in the form of conductivity. The conductivity values were derived from (Briaire, 2008). It was assumed that the conductivities of each domain were linear isotropic. The conductivity of the bone was chosen to be 0.02 as proposed by (Whiten, 2007) instead of 0.156 as proposed by (Briaire, 2008). An electrode carrier with 16 half-band electrode contacts modeling the HiFocus 1J was created (Fig. 3b).

The physiology of the auditory nerve fiber was modeled based on Smit et al. (2008). Each nerve fiber is composed by $k = 10$ sections, nodes 10 to 6 corresponded to the peripheral axon, node 5 to the soma and nodes 4 to 1 to the central axon (Fig. 3c). Fig. 3c shows the geometry of the most basal nerve fiber in a 2D plane of the model with the internode distances. The voltage distribution is sampled in each nerve section and is denoted as $V_i(k)$, where k denotes the section and i denotes the nerve fiber. For each nerve fiber the activation function is computed as the second derivative of the voltage distribution along the nerve axon (Rattay, 1999; Rattay et al., 2001):

$$D_i(k) = \frac{V_i(k-1) - 2V_i(k) + V_i(k+1)}{\Delta x^2}, \tag{1}$$

where Δx denotes the length of the neural elements.

The computational model of each node of the auditory nerve model is very similar to the one presented by Litvak et al. (2007). The spike timing is neglected and the spike count is summed for each time frame. To compute the number of neurons firing $N(x)$, each neuron is modeled independently. For a neuron i at position $X_i(k)$, the firing probability is equal to:

$$P(k) = \varnothing\left[\frac{|A_i(k)| - A_{thr_i}(k)}{A_{thr}(k)\cdot RS(k)}\right], \tag{2}$$

where $\varnothing$ is the cumulative normal distribution function, $A_{thr}(k)$ is the electrical activation required to reach the neuron's threshold, and RS is the neuron's relative spread (Bruce et al., 1999).

For the simulations, thresholds $A_{thr}(k)$ were assigned randomly from a log-normal distribution with the ratio of standard deviation to mean set to 0.3 (Litvak et al., 2007). For computational convenience, the mean of the threshold distributions was arbitrarily set at 0 dB relative to units of $A_i(k)$. As in Litvak et al. (2007), the *RS* of each neuron was chosen from a normal distribution with a mean of 0.0635 and a standard deviation of 0.04. The *RS* was not allowed to

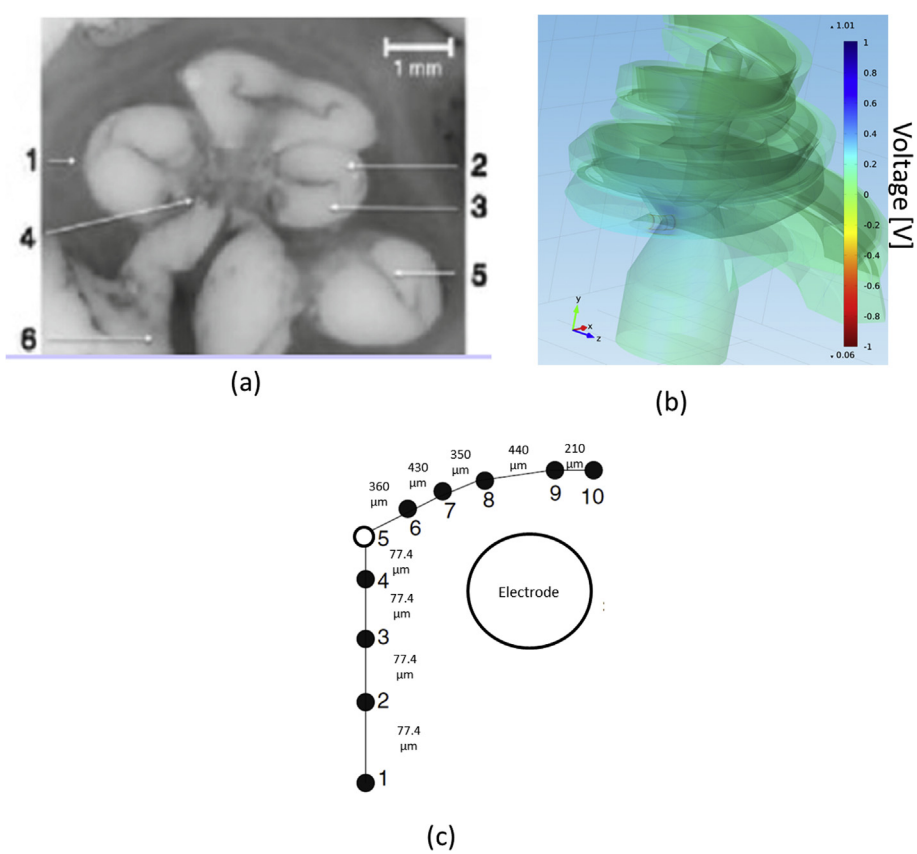

Fig. 3. a) Midmodiolar cross sectional image of a human cochlea. 1 Basilar membrane, 2 Modiolus, 3 Spiral ligament, 4 Scala vestibuli, 5 Scala tympani, 6 Limbus laminae spiralis; b) Visualization of the normalized voltage obtained from FEM for DC-VC stimulation using $\alpha = 0.5$ and $\sigma = -0.3$. The color bar indicates the magnitude of the voltage distribution from low (red) to high (blue) values.; c) Single auditory nerve fiber with k = 10 sections. (For interpretation of the references to colour in this figure legend, the reader is referred to the web version of this article.)

Please cite this article in press as: Nogueira, W., et al., Loudness and pitch perception using Dynamically Compensated Virtual Channels, Hearing Research (2016), http://dx.doi.org/10.1016/j.heares.2016.11.017

go below 0.03 or above 0.10. The model was applied to compute the summed neuronal activity $\sum N(x)$ under various configurations of DC-VC, i.e. for different values of the current steering coefficient α and the focusing coefficient σ.

The computational model was used to predict loudness for different DC-VC configurations. The model assumes that equivalent loudness is achieved by exciting the same total number of neural elements. Equivalent loudness was estimated for different values of α and σ modifying the current I that yielded a particular total neural activity $\sum N(x)$ across configurations. The total neural activity was fixed to 2000. Electrodes 7, 8, 9 and 10 were used to simulate different configurations of DC-VC stimulation. The stimulus configurations ranged from DC-VC with focused stimulation (σ = -0.30) to DC-VC with unfocused stimulation ($\sigma = 0.60$) using values of α ranging from 0.25 to 0.75. The simulation was run for different degrees of degeneration of the peripheral process by sampling the voltage distribution $V_i(k)$ at different nodes (from node $k = 10$ to node $k = 6$ as shown in Fig. 3c). The trimmed mean and standard deviation of the voltage distribution across the nodes was computed. It should be noted that the exact stimulus parameters (phase duration, polarity) are not important for the model which is only based on the activating function (second spatial derivative).

Fig. 4 presents the simulated currents delivering the same amount of neural activity N, with $N = 1$, 20, 2000 and 5000, for different values of σ and three values of α averaged across the different nodes. The model predicts a significant decrease in current with increasing values of σ. Moreover, the model predicts no effect of the current steering coefficient α on loudness perception. Fig. 3 shows that the percentage of current decrease with increasing σ for different amounts of neural activity N remains constant. Note that the range of the abscissa is different in each sub figure to emphasize the fact that the slope in the decrease of current is similar for different values of N. This means that for example the current contour for $N = 5000$ could be approximated shifting the current contour obtained for $N = 1$. This finding is in agreement with the work of Litvak et al. (2007) which reported that for relatively large distances between the neural fibers and the electrodes, the loudness contours can be essentially shifted.

1.1.2. Motivation

The outcomes from the computational model were used to formulate two hypotheses: 1) The current required to achieve comfortable loudness becomes lower with increasing values of σ; 2) Loudness does not depend on the current steering coefficient α using DC-VC stimulation mode. The purpose of experiment 1 was to assess the current levels required to achieve comfortable loudness with different values of the focusing parameter σ and the current steering parameter α.

1.1.3. Subjects

10 post-lingually deafened Advanced Bionics CII, HiRes90K or HiRes90K + CI users with a HiFocus 1J, Helix or Mid-Scala electrode arrays participated in the study. All subjects gave informed consent to the project as approved by the Medical University Hannover Institutional Review Board. The details for the study participants are given in Table 1.

1.1.4. Stimuli

All stimuli were composed of trains of charge-balanced, symmetric, anodic leading, biphasic pulses. The electrode attached to the case of the device on the implant was used as the distant ground. The reference stimuli consisted of DC-VC pulse trains (phase duration = 63.8 μs) presented simultaneously on electrodes 8 and 9 at a rate of 746 pulses per second (pps) with $\sigma = 0$ and a value of α set to 0.25, 0.5 or 0.9. A long phase duration was used to achieve comfortable loudness level without exceeding the

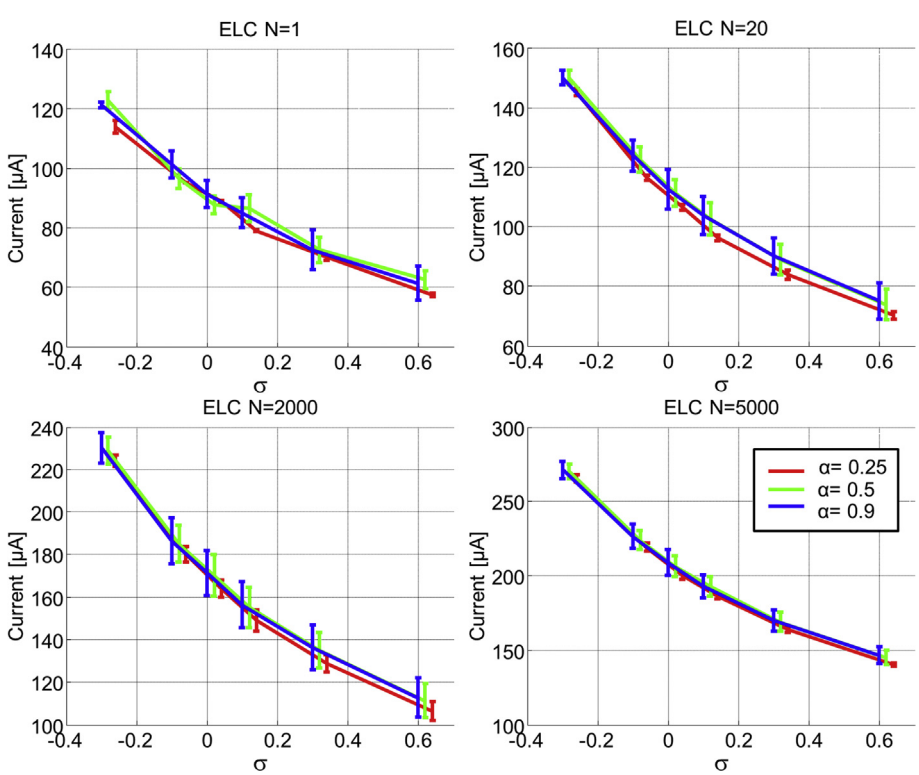

Fig. 4. Simulated currents delivering the same amount of neural activity ($N = 1$, 20, 2000 and 5000) or loudness for different values of σ and three values of α averaged across the different nodes (trimmed mean and the standard deviation).

Please cite this article in press as: Nogueira, W., et al., Loudness and pitch perception using Dynamically Compensated Virtual Channels, Hearing Research (2016), http://dx.doi.org/10.1016/j.heares.2016.11.017

Table 1
Subject details.

ID	Age	Duration of deafness (years)	Cause of deafness	Implant experience in years	Implant type and electrode
P1	26	0.09	Unknown	11	HiRes90k Helix
P2	45	32.67	Rubella	13	HiRes90k Helix
P3	44	0	Unknown	15	HiRes90k+ Mid-Scala
P4	53	26	Unknown	6	HiRes90k Helix
P5	51	3.75	Sudden Hearing Loss	14	CII HiFocus1J
P6	54	22.42	Cranial Fracture	5.5	HiRes90k Helix
P7	60	Unknown	Unknown	2.25	HiRes90k+ Mid-Scala
P8	46	0	Unknown	7	HiRes90K Mid-Scala
P9	67	0.01	Sudden Deafness	5.08	HiRes90k Helix
P10	64	0	Sudden Deafness	5.77	HiRes90k Helix

maximum compliance voltage of the device. The target stimulus consisted of a DC-VC pulse train of the same rate and the same α value as the reference stimuli but with a different σ. The value of σ for the target DC-VC stimulus was set to either −0.3, 0.3 or 0.6. Electrodes 8 and 9 were used as main electrodes, whereas electrodes 7 and 10 were used as compensating electrodes for both the reference and the target. All stimuli were delivered using the HRStream research interface (Advanced Bionics, Antwerp, Belgium). A short description of the HRStream research interface can be found in Nogueira and Buechner (2012).

1.1.5. Procedure

Loudness balancing was performed between the reference and the target stimulus for different values of σ. First, all target and DC-VC reference stimuli were set to a comfortable level by the CI user on a scale of 1–10, where 1 was equivalent to "very soft", 7 was equivalent to "comfortably loud" and 10 was equivalent to "extremely loud". Second, a reference and a target stimulus having the same value of α were loudness balanced. The loudness-balancing procedure consisted of repeatedly playing the reference stimulus followed by the target stimulus, the inter-stimulus interval was 500 ms. The reference and the target had a duration of 1 s. The CI users changed the level of the target using a knob interface (PowerMate, Griffin) to match the loudness between the target and the reference stimulus. The minimum resolution of the interface was 1 μA and the task was repeated two times starting from 10% above and below the target stimulus' comfortable loudness level. The loudness balancing procedure was repeated for different values of σ resulting in an equal loudness contour (ELC). Currents were obtained for $\alpha = 0.25$, 0.5 and 0.9. Subjects were instructed to adjust the level of the target to the reference.

1.1.6. Results

Fig. 5a presents the currents delivering equivalent loudness for the 10 CI users participating in the study in micro-Ampere (μA) units. Fig. 5b shows the data (20% trimmed mean of the individual data) as a function of α and the predicted currents by the model with the amount of neural elements fixed to $N = 5000$. This value of N was selected because it matched better the measured absolute current values required to achieve comfortable loudness in CI users. However, this parameter could be modified without affecting the relative changes in current for different values of α and σ, as shown in Fig. 4.

A two-way repeated measures analysis of variance (ANOVA) with factors σ and α revealed a significant effect of σ [$F(1.424,12.82) = 84.79$; $p < 0.0001$) but no significant effect of α [$F(1.016,9.142) = 1.426$; $p = 0.263$] on current required to maintain equal loudness (Fig. 5b). Because the sphericity assumption was violated a Greenhouse-Geisser correction was applied. No significant interaction effect between σ and α was observed [$F(1.018,9.160) = 1.446$; $p = 0.260$]. The averaged current across CI users and values of α was 336.58 μA, 245.20 μA, 197.43 μA and 163.35 μA for $\sigma = -0.3$, 0, 0.3 and 0.6 respectively. Therefore, the percentage of current savings with respect to the $\sigma = 0$ condition was −37.27%, 19.48% and 33.38% for $\sigma = -0.3$, 0.3 and 0.6, respectively.

Using Rom's method (Rom, 1990) to correct for family-wise Type-I error it was shown that each increase in the compensating coefficient σ caused a significant drop in current ($p < 0.0001$ for all pairs being compared). From these results, it can be concluded that unfocusing the field by increasing the value of σ can be used to reduce the current levels and therefore lower power consumption in CIs.

1.1.7. Discussion

Psychophysically measured equivalent loudness for different configurations of DC-VC stimulation show a dependency on the focusing coefficient σ but no dependency on the current steering coefficient α. Moreover, the experiments show that the focusing coefficient σ significantly effects loudness perception. The lower σ is, the more current is required to achieve equivalent loudness perception. The amount of current required to produce the same comfortable loudness as MP stimulation is increased by 37.27% for $\sigma = -0.3$ but reduced by 19.48% and 33.38% for $\sigma = 0.3$ and 0.6 respectively. The computational model of loudness also predicted a current reduction to achieve the same loudness percept with increasing values of the focusing coefficient σ.

Sound coding strategies based on current steering stimulation use the parameter α to linearly control the proportion of current delivered to two simultaneous stimulated electrodes (e. g. Nogueira et al., 2009). This linear control requires that loudness remains constant for different values of α to properly encode place pitch information (Frijns et al., 2009). Psychophysical experiments and outcomes from the computational model show no loudness effect

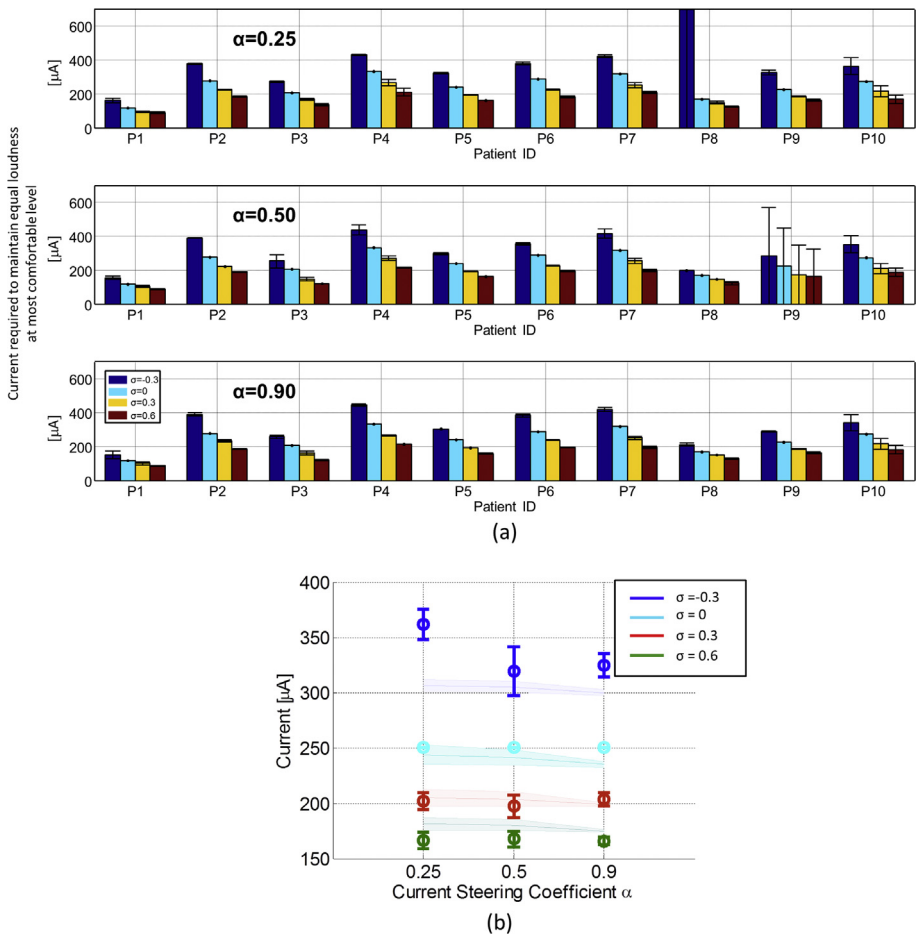

Fig. 5. a: Current required to obtain the same loudness perception across σ (−0.30, 0, 0.30 and 0.60) for different values of α (top panel: α = 0.25; central panel: α = 0.50; bottom panel: α = 0.90) for 10 CI users. The error bars indicate standard deviation. b: Current required to obtain the same loudness perception across σ (−0.30, 0, 0.30 and 0.60) for different values of α. The error bars indicate standard deviation. The 20% trimmed mean is used to summarize the results of all CI users. The predictions from the computational model configured with N = 5000 are given allowing the comparison between measured and predicted data.

for different values of the current steering coefficient α.

2. Experiment 2: pitch perception with Dynamically Compensated Virtual Channels

2.1. Pitch model

A pitch model was used to identify the mechanism of pitch changes for different configurations of DC-VC stimulation. For computational convenience the pitch model is based only on the activation function (Eq. (1)) and the geometrical position of the neurons. Therefore, no active neuron model was used during experiment 2. The model assumes that pitch is related to the peak of the activation function at nodes $k = 10, 9, 8, 7$ and 6 along the 10,000 nerve fibers, similar to the model proposed by Wu and Luo (2013). The model assumes that the peak location of the activation function will likely coincide with the location producing maximum neural activity. The peak location of each normalized pattern was defined as the geometrical location with the highest normalized amplitude of 1. The model was used to determine the values of α (for any value of $\sigma \neq 0$) that matched the peak location at $\alpha = 0.25$ and $\alpha = 0.75$ using MPVC (i.e. DC-VC with $\sigma = 0$). The peak location range is then defined as the difference between the value matched to $\alpha = 0.75$ and the value matched to $\alpha = 0.25$ when $\sigma = 0$. The peak range was computed by independently sampling the voltage distribution for nodes $k = 10, 9, 8, 7$ and 6.

Fig. 6 presents the trimmed mean and the standard deviation of

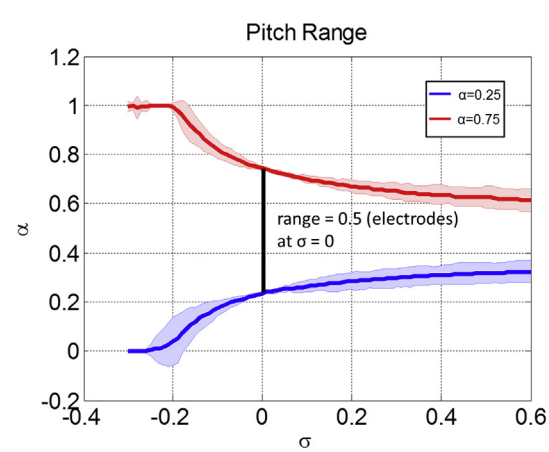

Fig. 6. Simulations of pitch perception using the computational model. The figure shows the α values for σ values ranging from −0.3 to 0.6 required to match the same pitch (centroid of the activation function) as $\alpha = 0.25$ and $\alpha = 0.75$ using $\sigma = 0$. The trimmed mean and standard deviation of the estimated pitch range at nodes 10, 9, 8, 7 and 6 was computed. The standard deviation is given as a shadow around the trimmed mean values. The black bar indicates the point where stimuli are pitched match to themselves.

Please cite this article in press as: Nogueira, W., et al., Loudness and pitch perception using Dynamically Compensated Virtual Channels, Hearing Research (2016), http://dx.doi.org/10.1016/j.heares.2016.11.017

the model predictions. It can be observed that with increasing σ, the peak location range, i.e. the space contained between the red and the blue curve is reduced. For focused stimulation with σ values below −0.2 the pitch range exceeds the physical electrodes, however in the figure the maximum value of 1 (for $\alpha = 0.75$) and the minimum value of 0 ($\alpha = 0$) is given. Interestingly the standard deviation across different nodes is small probably because the centroid of the voltage distribution does not change for the different nerve fiber nodes which is equivalent to different distances between the stimulating electrode and the nerve fibers.

Moreover, the computational model was used to assess the spatial selectivity produced by different DC-VC configurations. The spatial extent of the voltage distribution was estimated from the FEM study along the 10,000 nerve fibers. Similar to Wu and Luo (2013, 2016) the width at 50% of the peak voltage distribution amplitude was used to characterize the degree of spatial selectivity. The mean and standard deviation of the width was estimated simulating the voltage distribution at the 5 most peripheral nodes of the nerve fibers presented in Fig. 3c. The estimated width in [mm] (mean ± standard deviation) along the spiral ganglions for different values of α and σ is presented in Table 2.

From Table 2, it can be observed that increasing the value of σ causes an increase in the voltage distribution width. The effect of α on the width of the voltage distribution is much smaller.

In summary, results from the computational model show that with increasing σ, the peak location range is reduced and the width of the voltage distribution becomes larger.

2.2. Experiment 2.1: difference limen in the current steering coefficient α

2.2.1. Motivation

The goal of this experiment was to investigate whether focusing or unfocusing the electrical field through DC-VC stimulation had an effect on the discrimination of VCs. In DC-VC stimulation it is possible to focus or unfocus the voltage distribution. However, it is unknown its effects on the discrimination of virtual channels. In terms of applicability for sound coding strategies it is important to study whether DC-VC can cause detrimental effects relative to MPVCs as used in the F120 sound coding strategy.

2.2.2. Subjects

All subjects in Experiment 1 also participated in Experiment 2.1.

2.2.3. Stimuli

Stimuli were pulse trains of DC-VC stimulation with the same rate and pulse duration as in Experiment 1 (746 pps with each pulse having a 63.8 μs phase duration). The duration of the stimuli was fixed to 1 s. Electrodes 8 and 9 were used as the main electrodes whereas electrodes 7 and 10 were used as compensating electrodes. The values of the focusing coefficient σ were set to −0.3, 0, 0.3 or 0.6. All stimuli were loudness balanced. Current levels for α values intermediate to those directly loudness-balanced in the experiment were interpolated. All stimuli were delivered using the HRStream research interface.

Table 2
Modeled Spatial Selectivity (mean width and standard deviation in [mm]).

σ				
α	−0.3	0	0.3	0.6
0.25	8.8 ± 1.7	9.8 ± 1.4	10.3 ± 1.3	10.6 ± 1.3
0.5	8.8 ± 1.7	9.9 ± 1.4	10.5 ± 1.2	10.9 ± 1.1
0.75	8.8 ± 1.7	9.6 ± 1.5	10.1 ± 1.4	10.4 ± 1.4

2.2.4. Procedure

A 3-AFC 2down-1up procedure was used to estimate the just noticeable difference of α (jnd_α) for each value of σ (−0.3, 0, 0.3 and 0.6). In each trial two intervals contained the reference and one interval contained the target. The subject was instructed to identify which of the three sounds was different. The content of the intervals was randomized. The inter stimulus interval was set to 0.2 s. The reference stimulus was fixed at $\alpha = 0.25$ and the target stimulus was initialized at $\alpha = 0.9$. The step size was initially set to 0.2 and it was halved after each reversal until the minimum step size of 0.025 had been reached. At that point, the measurement phase started and it lasted for 4 reversals. Only the change from an up-phase to the next down-phase was counted as 1 reversal. The mean of the 4 last reversals were used to estimate the jnd_α. The procedure was implemented in Psylab (Hansen, 2006) where only the change from an up-phase to the next down-phase was counted as 1 reversal (i.e. one reversal comprises two "turning points").

All stimuli were presented at most comfortable level as measured in the previous experiment with a random level roving of ± 10% to reduce the effects of loudness cues on the measured discrimination. Training was provided to the CI users and consisted of two repetitions of the experiment with σ set to 0 to familiarize them with the task and the graphic user interface.

3. Results

Fig. 7 presents the jnd_α for 9 CI users and for different values of σ (−0.3, 0, 0.3, 0.6). CI user with ID P1 was not able to discriminate between $\alpha = 0.25$ and $\alpha = 0.90$ and therefore was dropped from this experiment. The jnd_α value for all CI users was obtained using the 20% trimmed mean.

The resulting data was analyzed using a one-way repeated measures ANOVA to test for the effect of processing scheme. The results of the ANOVA indicated a significant effect of σ on the jnd_α ($F(3, 32) = 2.881$, $p = 0.049$). A visual inspection suggests poorer discrimination of current steered places using DC-VC stimulation in focused mode (i.e. a negative σ) than in unfocused mode (i.e. a positive σ). Although the p-values for the differences between $\sigma = -0.3$ and 0, 0.3, and 0.6 are all 0.05 or less ($\sigma = -0.3$ vs $\sigma = 0$, $t(8) = 2.337$, $p = 0.048$; $\sigma = -0.3$ vs $\sigma = 0.3$, $t(8) = 2.311$, $p = 0.05$; $\sigma = -0.3$ vs $\sigma = 0.6$, $t(8) = 2.361$ $p = 0.046$), no significant

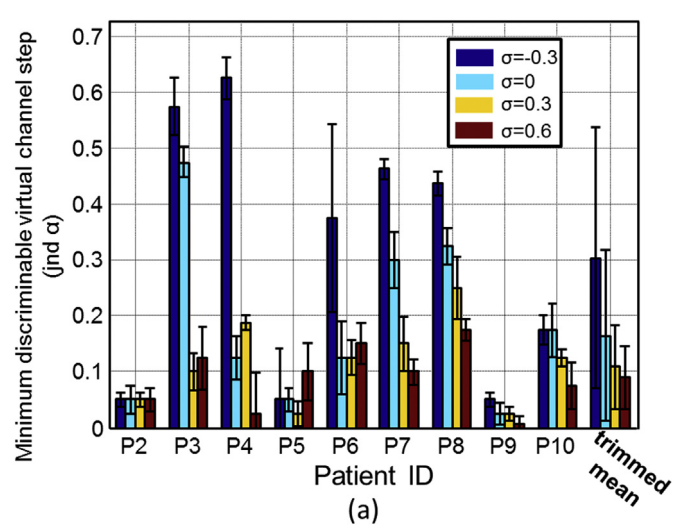

Fig. 7. jnd_α for different values of σ (−0.3, 0, 0.3 and 0.6) for 9 post-lingual CI users. The mean jnd_α value for all CI users was obtained using the 20% trimmed mean. The error bars indicate the standard deviation.

differences were detected after family-wise Type-I error control with Rom's (1990) method.

3.1. Experiment 2.2: pitch range of α

3.1.1. Motivation

The goal of this experiment was to investigate the range of current-steered pitch percepts that can be obtained with different values of the focusing coefficient σ. In terms of applicability for sound coding strategies, it is important to keep the pitch range constant for different configurations of DC-VC relative to MPVCs as used in the F120 sound coding strategy. Hence, it is expected that the overall sound perception delivered by the different configurations of DC-VC remains similar. The current-steered pitch range is defined as the difference in pitch obtained for $\alpha = 0.75$ and $\alpha = 0.25$. Pitch matching was performed between stimuli with $\sigma = 0$ at $\alpha = 0.75$ and $\alpha = 0.25$ with stimuli with $\sigma = -0.3$, 0.3 and 0.6 varying the value of α. The outcomes from the computational model predicted that increasing the value of the focusing coefficient σ causes a reduction in the required current steering range to cover the same pitch range.

3.1.2. Subjects

All subjects in Experiment 1 also participated in Experiment 2.2.

3.1.3. Stimuli

Stimuli were pulse trains of DC-VC stimulation with the same rate and phase duration as in the previous experiment. The reference DC-VC stimulus was configured either with $\alpha = 0.25$ or $\alpha = 0.75$ and with the focusing coefficient σ set to 0. The target DC-VC stimulus was configured with a variable value of α ranging from 0 until 1 and the focusing coefficient was set to either −0.3, 0.3 or 0.6. All stimuli were loudness balanced.

3.1.4. Procedure

The task consisted of a 2-AFC pitch matching procedure between the target and the reference stimulus. CI users had to report which of the two sounds, the target or the reference was higher in pitch. The task was repeated setting the start value of the target stimulus α to 0.1 and 0.9. The procedure was repeated for two reference stimuli having values of α set to 0.25 or 0.75 and for three target stimuli with σ set to −0.3, 0.3 or 0.6. The order of the presented reference and target stimuli was randomized. The step size was initially set to 0.2 and it was halved after each reversal until the minimum step size of 0.025 was reached. At that point, the measurement phase started and it lasted for 4 reversals. The mean of the 4 last reversals was used to estimate the jnd_α using the procedure described by Hansen (2006).

3.1.5. Results

Fig. 8 presents the values of α for different focusing coefficients σ (−0.3, 0.3 and 0.6) matched in pitch to the reference stimulus with α set to either 0.25 or 0.75 without focusing ($\sigma = 0$). 9 CI users (P2 to P10) participated in the study, again P1 was excluded from this experiment. In Fig. 8, the black line indicates the line with slope = 1, i.e. y = x. The blue, green, and red lines indicate the range for $\sigma = -0.3$, $\sigma = 0.3$, and $\sigma = 0.6$ respectively. A slope greater than 1 indicates an expanded place pitch range while a slope less than 1 indicates a compressed place pitch range. For most subjects, positive values of σ (red and green lines) produce a compressed pitch range, whereas a negative value σ (blue line) indicates an expanded place pitch range (e.g. P2, P3, P4, P8, P9).

The results presented in Fig. 8 are consistent with the prediction of the model. For some CI users (e.g. P3, P7, P9 and P10), the $\sigma = -0.3$ condition requires values of α close to 0 and 1 to produce the same pitch percept as the reference stimuli. This suggests that increasing the value of σ requires lower ranges of α to cover the same pitch range, which is also in agreement with model predictions.

It is important to note that the results in CI users show much more variability than can be explained by the model. The computational model of pitch showed little variability for different distances between the auditory nerve and the electrode position.

For each value of σ the pitch range of current steering α was estimated subtracting the value matched to $\alpha = 0.25$ using $\sigma = 0$ from the value matched to $\alpha = 0.75$ using $\sigma = 0$. The estimated pitch range of α for each CI user and for each focused coefficient σ is presented in Fig. 9.

The resulting data was compared using a one-way repeated measures ANOVA to test for the effect of the focusing coefficient σ on the current steered pitch range. The results of the ANOVA indicated a significant effect of σ on the range of α ($F(3,6) = 27.259$, $p = 0.001$). Using Rom's method to correct for family-wise type-I error, the range of α for $\sigma = -0.3$ was significantly lower than for $\sigma = 0.3$ ($p = 0.004$) and for $\sigma = 0.6$ ($p = 0.0001$). The range for $\sigma = 0.3$ was also significantly lower than for $\sigma = 0.6$ ($p = 1.75e\text{-}11$).

Finally, the number of discriminable stimuli within the range of α was estimated. This estimation was obtained dividing the pitch range of α by the jnd_α for each CI user and for each value of σ (Fig. 10).

The number of discriminable stimuli was obtained from the division of two variables, and its distribution is therefore, not normally or Gaussian distributed. For this reason, the hypothesis that the number of discriminable stimuli is independent of σ was performed using a bootstrapping method similar to the one described in the Appendix of Aronoff et al. (2016). The results were analyzed with a percentile bootstrap pairwise comparison with 20% trimmed means. To do this, a bootstrap distribution for each σ was obtained by resampling with replacement from the original measures.

2000 bootstrap distributions were generated (each with the same number of data points as the original distribution) for each pair σ. For each value of σ, the mean over each bootstrapped distribution was estimated. The mean of each bootstrapped distribution was then subtracted from each other. This mean difference was used to estimate the p-value. The p-value was estimated as the average number of times that this mean difference exceeded the measured difference divided by 2000. The null hypothesis on 0.05 chance level, i.e. 95% confidence interval was rejected if p was larger than 0.05. Results from this statistical analysis show no significant effects on the number of discriminable current steered steps, even without Type I error correction. The p-values ranged between 0.49 and 0.88. One reason for the lack of statistical significance in the number of discriminable current steered steps might be the large subject variability observed. For example, the results for subject P2 ranged from 16 steps to 3 steps.

3.2. Discussion

Predictions from the computational model as well as results from psychophysical experiments in CI users suggest that the range of values of α required to cover a fixed pitch range decreases with unfocused stimulation. Psychophysical experiments in CI users fail to detect a significant effect of the focusing coefficient σ in the discrimination of current steered channels. As a result, the total number of discriminable steps across different configurations of DC-VC (i.e. different values σ) remains almost constant.

For the CI users participating in the study, the trimmed mean discrimination of virtual channels (jnd_α) using MPVCs was 0.17 (ranging from 0.01 to 0.47). This range of values is in agreement with the data presented by Firszt et al. (2007) who showed that

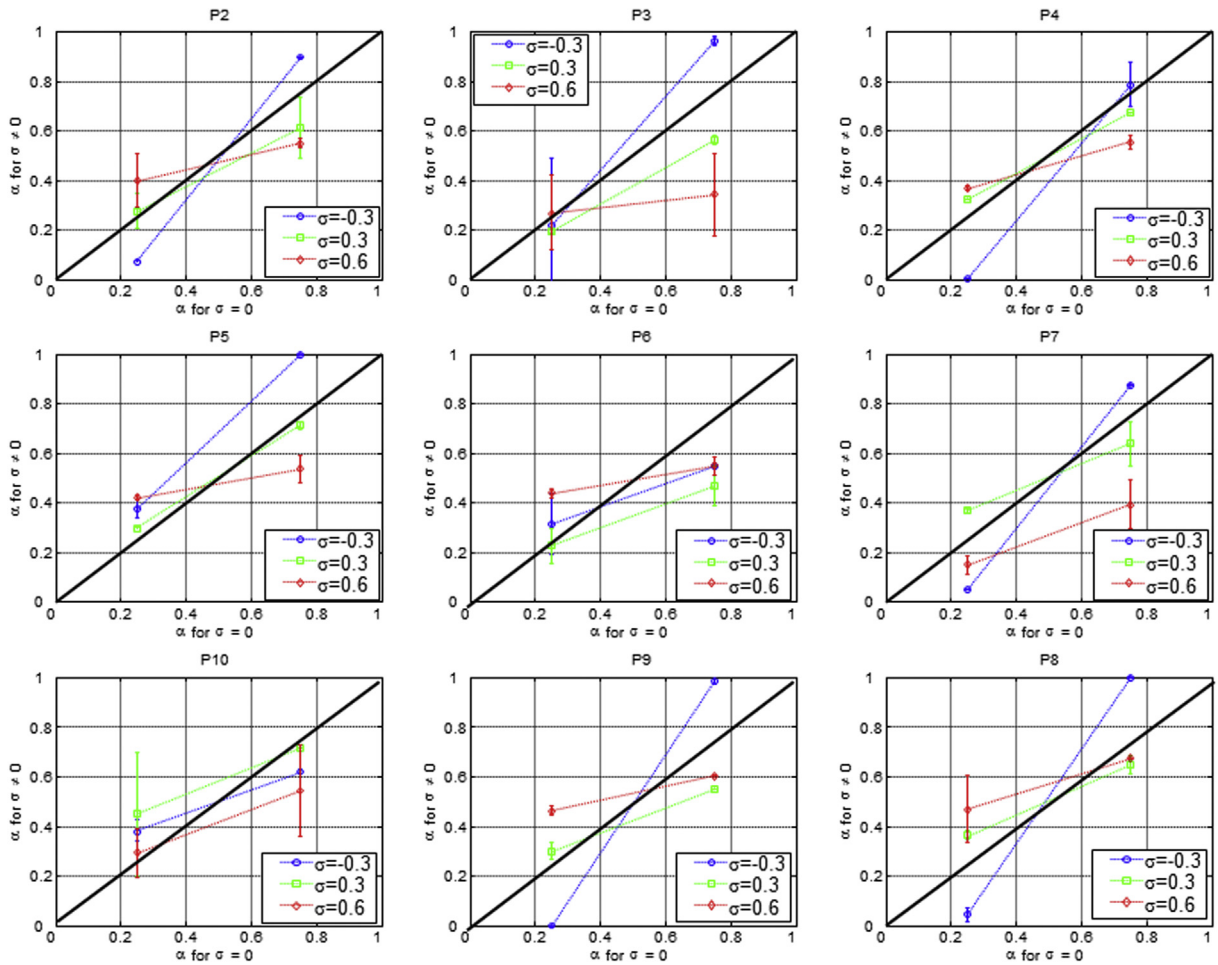

Fig. 8. Results of the current steering pitch range experiment for 9 CI users. The trimmed mean and the standard deviation are given for each value σ when the reference was set to $\alpha = 0.25$ or $\alpha = 0.75$. The black line indicates the line with slope = 1, i.e. y = x. Each color line indicates the range for each configuration of σ. If the slope of these lines is > 1 the range is expanded whereas if the slope is < 1 the range is compressed. (For interpretation of the references to colour in this figure legend, the reader is referred to the web version of this article.)

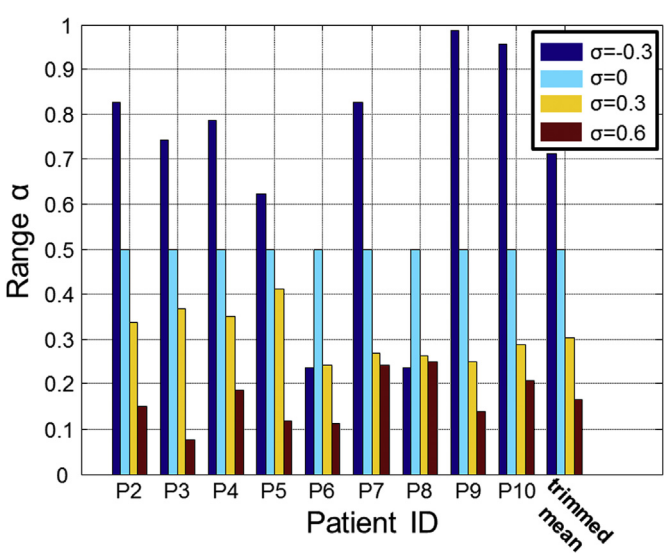

Fig. 9. Pitch range for different values of σ. The reference was σ = 0 for which the pitch range is 50% for all CI users. The mean range value of α for all CI users was obtained using the 20% trimmed mean.

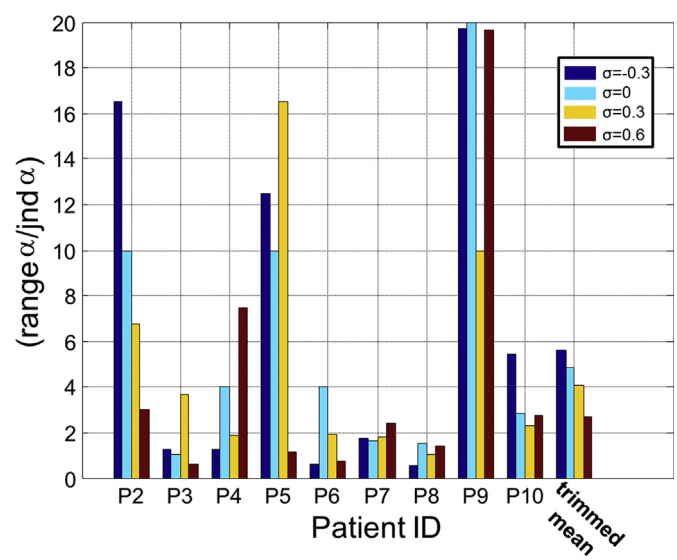

Fig. 10. Number of discriminable stimuli for different values of σ in 9 CI users as well as the 20% trimmed mean.

Please cite this article in press as: Nogueira, W., et al., Loudness and pitch perception using Dynamically Compensated Virtual Channels, Hearing Research (2016), http://dx.doi.org/10.1016/j.heares.2016.11.017

using MPVCs, for the apical and medial regions, more than 40% of subjects could discriminate two or more VCs. The psychophysical experiments presented in this manuscript show no effect of σ on the discrimination of virtual channels. These results seem to be in contradiction with the results presented by Landsberger and Srinivasan, (2009) that showed that current focusing improves current steering discrimination. This contradiction may be explained by the fact that DC-VC includes the current steering coefficient α in the flanking electrodes, whereas the QPVC does not. According to the computational model, peak shifts produced by DC-VC stimulation in unfocused mode are more exaggerated than in focused mode. This may help to compensate the potential negative effects of wider voltage distributions produced by unfocused stimulation to discriminate virtual channels.

Using DC-VC stimulation in unfocused mode, it is possible that the centroid of the voltage distribution shifts beyond the two main electrodes. At the extreme, if $\alpha = 0$ or $\alpha = 1$, the stimulation is a MPVC centered between 7 and 8 or 9 and 10. The pitch range experiment gives intuition on how to restrict the range of α such that it can be used in a sound coding strategy without exceeding the pitch (centroid) elicited by the two central electrodes.

The computational model of pitch perception has been useful to predict the effects of pitch range observed in CI users using different configurations of DC-VC stimulation. Essentially the model uses the centroid of the voltage distribution to determine the pitch elicited by each DC-VC configuration. One limitation of the model is that the results observed in CI users show more variability than the variability predicted by the pitch model. The model variability is obtained simulating different distances between the nodes of the auditory nerve and the electrodes, which in turn simulates auditory nerve dendrite degeneration. Additional measurements in CI users such as the relationship between focused stimulation and its relation to electrode modiolus distance (Long et al., 2014) can be used to individualize the auditory nerve model and try to explain the large inter-subject variability observed in CI users.

4. General discussion

This study has presented a new stimulation mode termed DC-VC that can be used to transmit virtual channels with varying degrees of focusing. The results of the study demonstrate that DC-VC can be used to reduce the amount of current required to achieve comfortable loudness without compromising the number of discriminable pitch steps between two adjacent electrodes.

The computational model used in this manuscript has been shown to predict relative loudness perception with different configurations of DC-VC. Such a model could be useful in a CI fitting software to predict the changes in amplitude required to maintain the most comfortable level when changing the parameters in the sound coding strategy. The model seems qualitatively consistent to predict comfort-level equal loudness contours measured with CI subjects. However, the model has limited capability to predict the absolute current values required by individual CI users. An additional limitation in the model is that the effect of different electrode-neuron distances has been simplified by performing predictions at different nodes of the peripheral process. The effects could be extended to more central nodes, as it is known that action potentials are also generated in the central axons (Rattay et al., 2001). This extension may lead to different estimates of the pitch ranges and the absolute current levels required to achieve comfort loudness sensation. A third limitation of the model is that it models shifts of activation on the cochlea and not place pitch discrimination which will presumably be dependent on more factors than place of stimulation. So far, the model has not been individualized to predict the loudness and pitch range of each CI user. However, the model has been parameterized such that the electrode positions, the cochlear size, as well as the degeneration of the auditory nerve can be adapted to each individual. Future studies could focus on how to adapt the different parameters of the model to predict loudness and pitch changes of individual CI users.

DC-VC can be incorporated into a sound coding strategy to provide power savings when the focusing parameter σ is larger than 0. Measurements in CI users and supporting models show that the number of discriminable VCs is not reduced by using unfocused stimulation ($\sigma > 0$). Results from the computational model suggest that the width of the voltage distribution using unfocused DC-VC is larger than that of focused stimulation. Thus, while two unfocused DC-VCs may be discriminable, there is likely to be large overlap in terms of current spread when all channels are activated in live mode. One suggestion to incorporate DC-VC stimulation mode in sound coding strategies is to use focused stimulation for soft input levels and unfocused stimulation for loud input sound levels. By doing so, at soft levels, where the stimulations levels are low, it is possible to deliver more focused stimulation without compromising power savings. For loud sounds however, large electrical stimulation currents are possible, and therefore power can be saved using unfocused DC-VC stimulation. In the normal hearing system it is known that tuning curves become broader as a function of increasing stimulus level (Ruggero et al., 2000; Oxenham and Simonson, 2006), therefore such a sound coding strategy based on DC-VC stimulation could provide also a better mimicking of the tuning curves observed in the human auditory system.

5. Conclusions

In conclusion, the main findings of this study are: 1) Predictions from a computational model and psychophysical experiments in CI users show that DC-VC can be used to reduce the current required to achieve comfortable loudness; 2) Psychophysical experiments in CI users show that unfocused DC-VC stimulation reduces the perceived pitch range. However, the number of discriminable virtual channels seems to remain constant independent of the degree of focusing applied. The computational model was able to predict the continuous reduction in pitch range obtained with unfocused stimulation. These findings are encouraging for the effective implementation of the DC-VC mode in a sound coding strategy to reduce power consumption, without compromising the amount of discriminable virtual channels.

Acknowledgements

The authors would like to thank the subjects who have participated in the experiments. The authors would also like to thank Amy Stein and Chen Chen from Advanced Bionics for the support in the preparation of the manuscript. This work was supported by the German Research Foundation (DFG) Cluster of Excellence EXC 1077/1 “Hearing4all”, Advanced Bionics and the NIH/NIDCD (R01 DC012152, PI: Landsberger).

References

Aronoff, J.M., Stelmach, J., Padilla, M., Landsberger, D.M., 2016. Interleaved processors improve cochlear implant patients' spectral resolution. Ear Hear 37, e85–e90.

Berenstein, C.K., Mens, L.H., Mulder, J.J., Vanpoucke, F.J., 2008. Current steering and current focusing in cochlear implants: comparison of monopolar, tripolar, and virtual channel electrode configurations. Ear Hear 29 (2), 250–260.

Bierer, J.A., Faulkner, K.F., 2010. Identifying cochlear implant channels with poor electrode-neuron interface: partial tripolar, single-channel thresholds and psychophysical tuning curves. Ear Hear 31, 247–258.

Bierer, J.A., Litvak, L., 2016. Reducing channel interaction through cochlear implant

programming may improve speech perception: current focusing and channel deactivation. Trends Hear 20.
Bierer, J.A., Middlebrooks, J.C., 2002. Auditory cortical images of cochlear-implant stimuli: dependence on electrode configuration. J. Neurophysiol. 87, 478–492.
Bonham, B.H., Litvak, L.M., 2008. Current focusing and steering: modeling, physiology, and psychophysics. Hear Res. 242 (1–2), 141–153.
Briaire, J.J., 2008. Cochlear Implants from Model to Patients. Thesis. Universiteit Leiden, ISBN 978-90-9023555-4.
Briaire, J.J., Frijns, J.H., 2010. Field patterns in a 3D tapered spiral model of the electrically stimulated cochlea. Hear Res. 148, 18–30.
Briggs, R.J.S., Eder, H.C., Seligman, P.M., Cowan, R.S.C., Plant, K.L., Dalton, J., Money, D.K., Patrick, J.F., 2008. Initial clinical experience with a totally implantable cochlear implant research device. Otol. Neurotol. 29, 114–119.
Bruce, I.C., White, M.W., Irlicht, L.S., O'Leary, S.J., Dynes, S., Javel, E., Clark, G.M., 1999. A stochastic model of the electrically stimulated auditory nerve: single pulse response. IEEE Trans. Biomed. Eng. 46, 617–629.
Busby, P.A., Battmer, R.D., Pesch, J., 2008. Electrophysiological spread of excitation and pitch perception for dual and single electrodes using the nucleus freedom cochlear implant. Ear Hear 29, 853–864.
Buechner, A., Brendel, M., Krüeger, B., Frohne-Büchner, C., Nogueira, W., Edler, B., Lenarz, T., 2008. Current steering and results from novel speech coding strategies. Otol. Neurotol. 29 (2), 203–207.
Donaldson, G.S., Kreft, H.A., Litvak, L., 2005. Place-pitch discrimination of single- versus dual-electrode stimuli by cochlear implant users (L). J. Acoust. Soc. Am. 118, 623–626.
Fu, Q.J., Nogaki, G., 2005. Noise susceptibility of cochlear implant users: the role of spectral resolution and smearing. J. Assoc. Res. Otolaryngol. 6, 19–27.
Fielden, C.A., Kluk, K., McKay, C.M., 2013. Place specificity of monopolar and tripolar stimuli in cochlear implants: the influence of residual masking. J. Acoust. Soc. Am. 133, 4109–4123.
Firszt, J.B., Koch, D.B., Downing, M., Litvak, L., 2007. Current steering creates additional pitch percepts in adult cochlear implant recipients. Otol. Neurotol. 28, 629–636.
Frijns, P.J.H.M., Kalkman, R.K., Vanpoucke, F.J., Bongers, J.S., Briaire, J.J., Johan, P., Kalkman, R.K., Vanpoucke, F.J., 2009. Simultaneous and non-simultaneous dual electrode stimulation in cochlear implants: evidence for two neural response modalities. Acta Otolaryngol. 129 (4), 433–439.
Frijns, J.H., Dekker, D.M., Briaire, J.J., 2011. Neural excitation patterns induced by phased-array stimulation in the implanted human cochlea. Acta Otolaryngol. 131, 362–370.
Hansen, M., 2006. Lehre und Ausbildung in Psychoakustik mit psylab: freie Software für psychoakustische Experimente. Fortschr. Akust. DAGA 06, 591–592.
Henry, B.A., McKay, C.M., McDermott, H.J., Clark, G.M., 2000. The relationship between speech perception and electrode discrimination in cochlear implantees. J. Acoust. Soc. Am. 108, 1269–1280.
Hughes, M.L., Stille, L.J., Baudhuin, J.L., Goehring, J.L., 2013. ECAP spread of excitation with virtual channels and physical electrodes. Hear Res. 306, 93–103.
Kalkman, R.K., Briaire, J.J., Frijns, J.H.M., 2014. Current focussing in cochlear implants: an analysis of neural recruitment in a computational model. Hear Res. 322, 89–98.
Landsberger, D.M., Srinivasan, A.G., 2009. Virtual channel discrimination is improved by current focusing in cochlear implant recipients. Hear. Res. 254 (1–2), 34–41.
Landsberger, D., Galvin, J.J., 2011. Discrimination between sequential and simultaneous virtual channels with electrical hearing. J. Acoust. Soc. Am. 130, 1559.
Landsberger, D.M., Padilla, M., Srinivasan, A.G., 2012. Reducing current spread using current focusing in cochlear implant users. Hear Res. 284, 16–24.
Litvak, L.M., Spahr, A.J., Emadi, G., 2007. Loudness growth observed under partially tripolar stimulation: model and data from cochlear implant listeners. J. Acoust. Soc. Am. 122 (2), 967–981.
Litvak L. M. and Marzalek M. S. (2012). Systems and methods for controlling a width of an excitation field created by current applied by a cochlear implant system, WO 20150328457 A2, PCT/US2013/072492, US Patent, December.
Loizou, P.C., 1998. Mimicking the human ear. IEE Signal Process. Mag. 15 (5), 101–130. Sep. 1998.
Long, C.J., Holden, T.A., McClelland, G.H., Parkinson, W.S., Shelton, C., Kelsall, D.C., Smith, Z.M., 2014. Examining the electro-neural interface of cochlear implant users using psychophysics, CT scans, and speech understanding. J. Assoc. Res. Otolaryngol. 15, 293–304.
Luo, X., Landsberger, D.M., Padilla, M., Srinivasan, A.G., 2010. Encoding pitch contours using current steering. J. Acoust. Soc. Am. 128, 1215–1223.
Luo, X., Padilla, M., Landsberger, D.M., 2012. Pitch contour identification with combined place and temporal cues using cochlear implants. J. Acoust. Soc. Am. 131, 1325–1336.
Mertens, G., Hofkens, A., Punte, A.K., De Bodt, M., Van de Heyning, P., 2015. Hearing performance in single-sided deaf cochlear implant users after upgrade to a single-unit speech processor. Otol. Neurotol. 36 (1), 51–60, 2015 Jan.
McKay, C.M., Remine, M.D., McDermott, H.J., 2001. Loudness summation for pulsatile electrical stimulation of the cochlea: effects of rate, electrode separation, level, and mode of stimulation. J. Acoust. Soc. Am. 110, 1514–1524.
Nogueira, W., Litvak, L.M., Edler, B., Ostermann, J., Büchner, A., 2009. Signal processing strategies for cochlear implants using current steering. EURASIP J. Adv. Signal Process. ID 531213.
Nogueira, W., Buechner, A., 2012. Conveying low frequency information through analog electrical stimulation in cochlear implants. In: Proceedings of the 20th European Signal Processing Conference (EUSIPCO), pp. 509–513.
Nogueira, W., Schurzig, D., Penniger, R., Büchner, A., Würfel, W., 2016. Validation of a cochlear implant patient specific model of the voltage distribution in a clinical setting. Front. Bioeng. Biotechnol. 4, 84.
Oxenham, A.J., Simonson, A.M., 2006. Level dependence of auditory filters in nonsimultaneous masking as a function of frequency. J. Acoust. Soc. Am. 119 (1), 444–453.
Padilla, M., Landsberger, D.M., 2014. Loudness summation using focused and unfocused stimulation. J. Acoust. Soc. Am. 135, EL102–108.
Rattay, F., 1999. The basic mechanism for the electrical stimulation of the nervous system. Neuroscience 89, 335–346.
Rattay, F., Leao, R.N., Felix, H., 2001. A model of the electrically excited human cochlear neuron. II. Influence of the three-dimensional cochlear structure on neural excitability. Hear. Res. 153, 64–79.
Rom, D.M., 1990. A sequentially rejective test procedure based on a modified Bonferroni inequality. Biometrika 77, 663–665.
Ruggero, M.A., Narayan, S.S., Temchin, A.N., Recio, A., 2000. Mechanical bases of frequency tuning and neural excitation at the base of the cochlea: comparison of basilar-membrane vibrations and auditory-nerve-fiber responses in chinchilla. Proc. Natl. Acad. Sci. U. S. A. 97, 11744–11750.
Shannon, R.V., Zeng, F.G., Kamath, V., Wygonski, J., Ekelid, M., 1995. Speech recognition with primarily temporal cues. Science 270, 303–304.
Shannon, R.V., Fu, Q.-J., Galvin III, J.J., 2004. The number of spectral channels required for speech recognition depends on the difficulty of the listening situation. Acta Otolaryngol. (Suppl. 552), 1–5.
Smit, J.E., Hanekom, T., Hanekom, J.J., 2008. Predicting action potential characteristics of human auditory nerve fibres through modification of the Hodgkin-Huxley equations. S. Afr. J. Sci. 104, 284–292.
Smith, Z.M., Parkinson, W.S., Long, C.J., 2013. Multipolar current focusing increases spectral resolution in cochlear implants. In: IEEE Engineering in Medicine and Biology Society.
Snel-Bongers, J., Briaire, J.J., van der Veen, E.H., Kalkman, R.K., Frijns, J.H., 2013. Threshold levels of dual electrode stimulation in cochlear implants. J. Assoc. Res. Otolaryngol. 14 (5), 781–790.
Spelman, F.A., Pfingst, B.E., Clopton, B.M., Jolly, C.N., Rodenhiser, K.L., 1995. Effects of electrical current configuration on potential fields in the electrically stimulated cochlea: field models and measurements. Ann. Otol. Rhinol. Laryngol. Suppl. 166, 131–136.
Srinivasan, A.G., Shannon, R.V., Landsberger, D.M., 2012. Improving virtual channel discrimination in a multi-channel context. Hear Res. 286 (1–2), 19–29.
Srinivasan, A.G., Padilla, M., Shannon, R.V., Landsberger, D.M., 2013. Improving speech perception in noise with current focusing in cochlear implant users. Hear Res. 299C, 29–36.
Wilson, B.S., Finley, C.C., Lawson, D.T., Wolford, R.D., Eddington, D.K., Rabinowitz, W.M., 1991. Better speech recognition with cochlear implants. Nature 352, 236–238.
Whiten, D.M., 2007. Electro Anatomical Models of the Cochlear Implant. Doctoral Thesis. Div. Health Sci. & Tech, Massachusetts Institute of Technology, Cambridge, 2007.
Wouters, J., Mcdermott, H.J., Francart, T., 2015. Sound coding in cochlear implants: from electric pulses to hearing. IEEE Signal Process. Mag. 32, 67–80.
Wu, C.C., Luo, X., 2013. Current steering with partial tripolar stimulation mode in cochlear implants. J. Assoc. Res. Otolaryngol. 14 (2), 213–231.
Wu, C.C., Luo, X., 2016. Excitation patterns of standard and steered partial tripolar stimuli in cochlear implants. J. Assoc. Res. Otolaryngol. 17 (2), 145–158.
Zeng, F.G., Rebscher, S., Harrison, W., Sun, X., Feng, H., 2008. Cochlear implants: system design, integration, and evaluation. IEEE Rev. Biomed. Eng. 1, 115–142.

Please cite this article in press as: Nogueira, W., et al., Loudness and pitch perception using Dynamically Compensated Virtual Channels, Hearing Research (2016), http://dx.doi.org/10.1016/j.heares.2016.11.017